Observation of the Power Spectrum of Ocean Waves Using a Cloverleaf Buoy

HISASHI MITSUYASU, FUKUZO TASAI, TOSHIRO SUHARA, SHINJIRO MIZUNO, MAKOTO OHKUSU, TADAO HONDA AND KUNIO RIKIISHI[1]

Research Institute for Applied Mechanics, Kyushu University, Fukuoka, Japan

(Manuscript received 4 June 1979, in final form 5 September 1979)

ABSTRACT

The power spectra of typical sets of ocean wave data obtained in the open ocean using a cloverleaf buoy are analyzed to determine an idealized form for the spectrum of ocean surface waves. It is shown that most of the single-peaked spectra observed in a generation area can be described well by the spectral form of the JONSWAP type. Two parameters α and γ characterizing the spectral form are calculated for each spectrum measured. Their relations to the dimensionless peak frequency $\hat{f}_m$ ($= f_m U/g$) are then determined. These relations are further converted into fetch relations for α and γ through a relation between $\hat{f}_m$ and a dimensionless fetch $\tilde{F}$ ($= gF/U^2$).

Another spectral form proposed by Toba (1978) is examined and shown to fit as well to the observed spectra at high frequencies. This fact shows quasi-equivalence of the JONSWAP spectrum and Toba's spectrum in the high-frequency range. On the basis of the agreements of both spectral forms at high frequencies, properties of the dimensionless constant α' in Toba's spectrum are examined. It is shown that α' depends very weakly on the dimensionless fetch $\tilde{F}$.

1. Introduction

This paper is a sequel to our earlier paper (Mitsuyasu *et al.*, 1975), in which we studied the directional wave spectrum of ocean wave data measured by using a cloverleaf buoy. In the previous paper, however, the analysis and discussions were mainly focused on the form of the angular distribution function and only qualitative discussions were made of the power spectrum. The purpose of the present paper is to determine a similarity form for the power spectrum of wind waves in the open ocean by using ocean wave data measured with the cloverleaf buoy.

For fully developed wind waves in the open ocean, Pierson and Moskowitz (1964) proposed a form of the power spectrum (PM spectrum), which shows the fetch-independent form

$$\phi(f) = \alpha g^2 (2\pi)^{-4} f^{-5} \exp\left[-\frac{5}{4}\left(\frac{f}{f_m}\right)^{-4}\right], \quad (1)$$

where $\alpha = 8.10 \times 10^{-3}$ and

$$f_m = (2\pi)^{-1}(4\beta/5)^{1/4} g U_{19.5}^{-1} \quad (2)$$

where $\beta = 0.74$ and $U_{19.5}$ is the wind speed at the height $z = 19.5$ m.

On the other hand, for fetch-limited wind waves in the ocean, Hasselmann *et al.* (1973) proposed the JONSWAP spectrum,

$$\phi(f) = \alpha g^2 (2\pi)^{-4} f^{-5} \times \exp\left[-\frac{5}{4}\left(\frac{f}{f_m}\right)^{-4}\right] \gamma^{\exp[-(f/f_m-1)^2/2\sigma^2]}, \quad (3)$$

where α and f_m are fetch-dependent scale parameters of the wave spectrum, and γ and σ are shape parameters discussed below.

Owing to the large scatter of the measured shape parameters, they determined only the following mean JONSWAP values for the shape parameters:

$$\left.\begin{aligned} \gamma &= 3.3 \\ \sigma &= \begin{cases} \sigma_a = 0.07, & f \leq f_m \\ \sigma_b = 0.09, & f > f_m \end{cases} \end{aligned}\right\}. \quad (4)$$

The shape parameter γ is sometimes called the "peak enhancement factor," because it represents the ratio of the maximum spectral energy to the maximum of the corresponding PM spectrum at the same frequency f_m. Evidently, the JONSWAP spectrum reduces to the PM spectrum for $\gamma = 1$ except for the fetch-dependent scale parameters α and f_m, but for $\gamma > 1$ the JONSWAP spectrum has much more concentrated spectral energy near the spectral peak as compared to the PM spectrum.

According to our previous study, some of the power spectra measured in the open ocean showed

[1] Present affiliation: Institute of Geoscience, Hirosaki University, Hirosaki, Japan.

0022-3670/80/020286-11$06.75

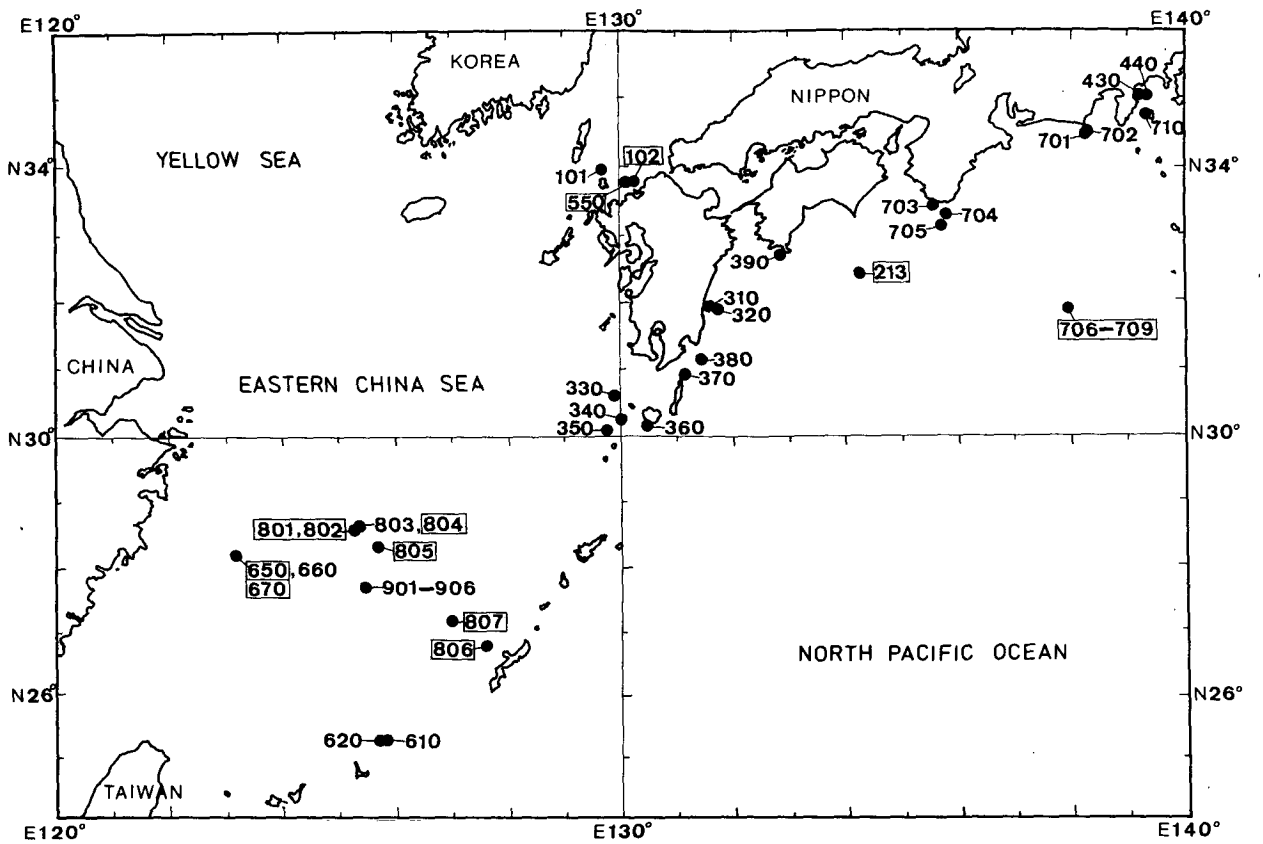

FIG. 1. Locations of the wave observations. Boxed values are used for the present study.

quite a similar form to that of the PM spectrum, but some others showed much higher concentration of the spectral energy than that of the PM spectrum. Furthermore, the concentration of the spectral energy of the wind waves seemed to depend on the dimensionless fetch $\tilde{F}$ ($\equiv gF/U^2$), though a definite relation between the spectral form and the dimensionless fetch had not been determined. In order to obtain an idealized form for the power spectrum of ocean waves, we try, in this paper, to extend the JONSWAP spectrum by determining the accurate fetch relations for the shape parameters α and γ.

In a sense, the JONSWAP spectrum can be considered as the spectral form for partially developed ocean waves (ocean waves at the developing stage) as discussed recently by Pierson (1977). A determination of the idealized spectral form for partially developed ocean waves should be useful since it is frequently encountered in the open ocean.

2. Wave data and spectra

a. Wave data

The wave data used in the present study were obtained during a period from 1971 to 1976 by using a cloverleaf buoy. Sites of the wave observations

TABLE 1. Information summary. Time: Japan Standard (starting time for wave recording); U_e, wind speed estimated from f_m and E using Eq. (12); $\tilde{F}$ ($\equiv gF/U_e^2$), the dimensionless fetch estimated from the fetch relation Eq. (9).

Data no.	Date	Time	Wind data: Direction	Wind data: U (m s^{-1})	Wind data: U_e (m s^{-1})	$\tilde{F}$ ($\times 10^4$)
213	'71-12-29	1405	NE	7.0	6.5	2.94
550	'73-2-19	1100	NNE	6.5	8.2	2.93
651	'73-5-24	1418	NE	9.0	8.1	1.64
672	'76-6-3	1550	E	9.0	7.8	0.74
707	'74-2-13	0941	WNW	10.0	13.2	0.46
708	'74-2-13	1008	WNW	10.0	11.1	0.85
709	'74-2-13	1315	WNW	9.5	11.8	0.85
801	'75-2-16	1743	N	11.0	8.1	3.14
802	'75-2-16	1802	N	11.0	8.8	2.27
804	'75-2-19	0906	N	14.0	11.1	1.20
805	'75-2-19	1521	N	14.0	10.3	1.51
806*	'75-2-23	1110	NW	7.0	6.9	6.97
807*	'75-2-23	1617	NNW	5.5	5.3	12.70
102	'76-10-20	0805	SSW	12.0	10.7	0.18

* Wind speeds 10–15 m s^{-1} continued ~70 h until 1000 JST 23 February 1975. Then the wind speed decreased gradually to the values shown in this table.

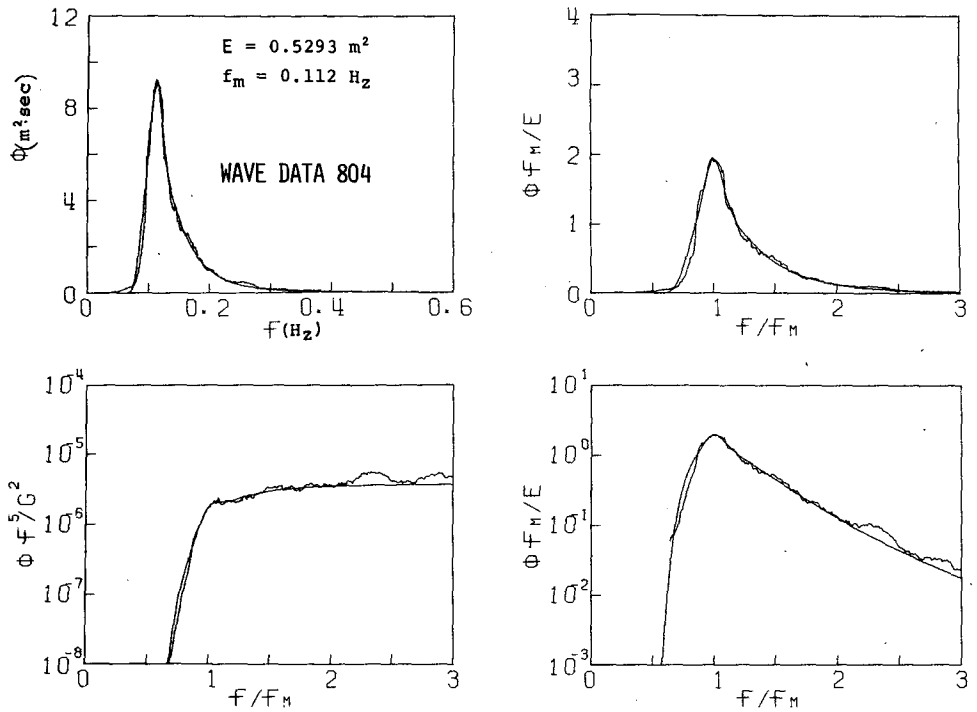

FIG. 2. Power spectrum and its normalized form for ocean wave data set No. 804. The smooth curve in each figure is a spectral form given by Eq. (3) with the best-fit values of α and γ.

are shown in Fig. 1, and details of the observations are summarized in Table 1. The dimensionless fetch $\tilde{F}$ is determined by a method to be discussed in Section 4.

From 67 wave data sets of ~1 h duration, 14 sets were selected and analyzed to determine the detailed characteristics of the power spectra of ocean waves. The wave data selected satisfy the following criteria: 1) waves were generated by an approximately constant wind of long duration (at least longer than 10 h); 2) dominant swells did not coexist with wind waves; and, accordingly, 3) wave spectra were of a single-peaked form. The duration times for the present data were generally larger than the minimum duration ($t_{\min}$) required to produce a steady state for given dimensionless fetch $\tilde{F}$.

b. Wave spectra

Computation of the spectra was carried out for the same conditions as that described in the previous study (Mitsuyasu *et al.*, 1975):

Sampling interval of the data: $\Delta t = 0.4$ s
Data points (for one subsample): $N = 2048$
Sample length (for one subsample): $T_N \approx 13.6$ min
Nyquist frequency: $f_N = 1.25$ Hz
Spectral analysis: FFT method
Elementary frequency bandwidth: $\Delta f_0 = 1.22 \times 10^{-3}$ Hz
Spectral filter (triangular): $\Delta f_c = 3.66 \times 10^{-2}$ Hz
Equivalent degree of freedom (for one subsample): $\nu = 60$

Usually three subsamples are used for each data set. Therefore, the equivalent degrees of freedom for the measured power spectra are approximately 180.

Amplitude response of the cloverleaf buoy is constant up to ~0.3 Hz and decreases gradually with increasing frequency. Measured wave spectra are corrected by using the amplitude response function determined experimentally in a large wave tank. The wave spectra after the correction are considered to be accurate at least up to 0.5 Hz, beyond which the buoy shows complicated response due to its special geometrical configuration. Since the spectral peak frequency f_m of our measured spectra lies in a range 0.1 ~ 0.2 Hz, the measured spectra are accurate at least up to $2.5f_m$.

3. Preliminary considerations

a. Universal relations for wind wave parameters

We have previously derived the following fetch-dependent relations for the wind wave energy E and for the spectral peak frequency f_m by using the spectral data of fetch-limited wind waves in a laboratory tank as well as in a bay (Mitsuyasu, 1968):

$$\frac{gE^{1/2}}{u_*^2} = 1.31 \times 10^{-2}\left(\frac{gF}{u_*^2}\right)^{0.504}, \qquad (5)$$

$$\frac{u_* f_m}{g} = 1.00\left(\frac{gF}{u_*^2}\right)^{-0.330}, \tag{6}$$

where u_* is a friction velocity of the wind, g the gravitational acceleration and F a fetch. Relations (5) and (6) are modified as follows by approximating the constants as $0.504 \rightarrow 1/2$, $0.330 \rightarrow 1/3$, converting the friction velocity u_* into the wind speed U at 10 m height by

$$u_*^2 = C_D U^2, \tag{7}$$

and assuming the drag coefficient as $C_D = 1.6 \times 10^{-3}$;

$$\tilde{E}^{1/2} = 5.24 \times 10^{-4}\tilde{F}^{1/2}, \tag{8}$$

$$\tilde{f}_m = 2.92\tilde{F}^{-1/3}, \tag{9}$$

where $\tilde{E}$, $\tilde{F}$ and $\tilde{f}_m$ represent the dimensionless variables

$$\tilde{E} = g^2E/U^4, \quad \tilde{F} = gF/U^2 \quad \text{and} \quad \tilde{f}_m = Uf_m/g. \tag{10}$$

As will be shown later these relations are quite similar to those obtained by Hasselmann *et al.* (1973). By eliminating the dimensionless fetch $\tilde{F}$ from (8) and (9), we obtain an important relation between the dimensionless wave energy $\tilde{E}$ and the dimensionless frequency $\tilde{f}_m$ at the spectral peak:

$$\tilde{E} = 6.84 \times 10^{-6}\tilde{f}_m^{-3}. \tag{11}$$

A relation of this form was originally proposed by Toba (1972, 1978) as a universal relation for growing wind waves. As pointed out by Toba (1972) the relation (11) is not necessarily restricted to fetch-limited wind waves; a quite similar relation is obtained from Wilson's (1965) empirical formula, which is valid for very large dimensionless fetch $\tilde{F}$. The dimensional form of (11) becomes

$$Ef_m^3 = 6.84 \times 10^{-6} gU. \tag{12}$$

Relation (12) is used for estimating from the data of E and f_m the effective wind speed U_e in the generation area.

b. Various parameters in the JONSWAP spectrum

Hasselmann *et al.* (1973) determined scale parameters of the JONSWAP spectrum (3) as

$$\alpha = 7.6 \times 10^{-2}\tilde{F}^{-0.22}, \tag{13}$$

$$\tilde{f}_m = 3.5 \times \tilde{F}^{-0.33}. \tag{14}$$

The fetch relation for the wave energy E is

$$\tilde{E} = 1.6 \times 10^{-7}\tilde{F}. \tag{15}$$

The constants in the relations (14) and (15) are somewhat different from those in our corresponding relations (9) and (8). The differences are attributed mainly to the different assumptions for the drag coefficient C_D in converting u_* into U, i.e.,

$C_D = 1.0 \times 10^{-3}$ [Hasselmann *et al.* (1973)].

$C_D = 1.6 \times 10^{-3}$ [present study].

Due to the large scatter in the values of γ, the fetch relation for the shape parameter γ was not derived

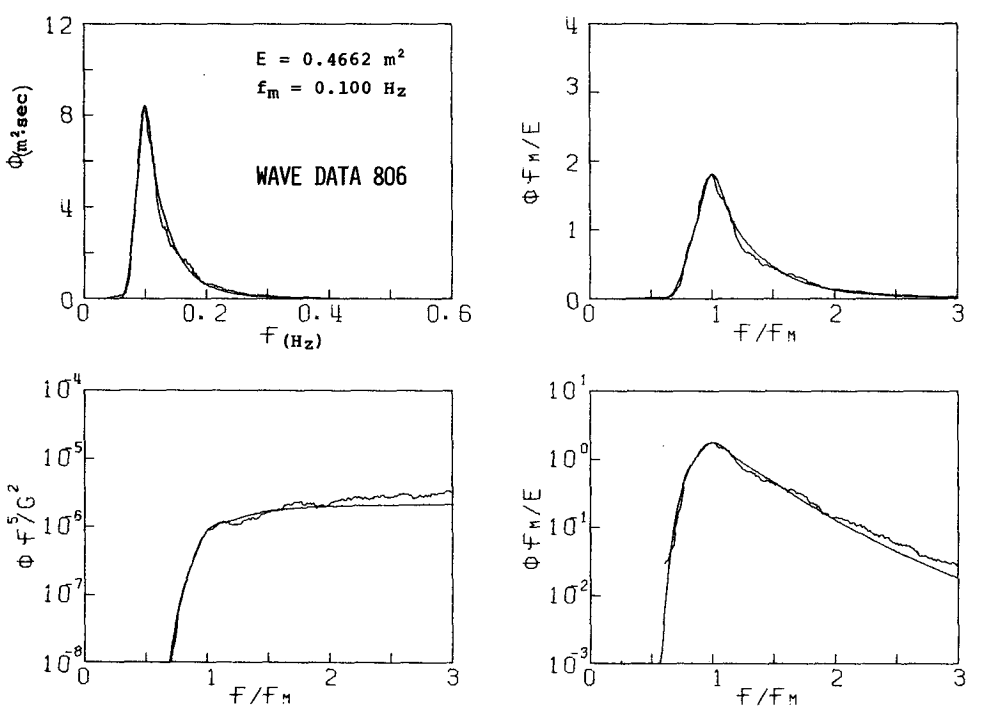

FIG. 3. As in Fig. 2 except for ocean wave data set No. 806.

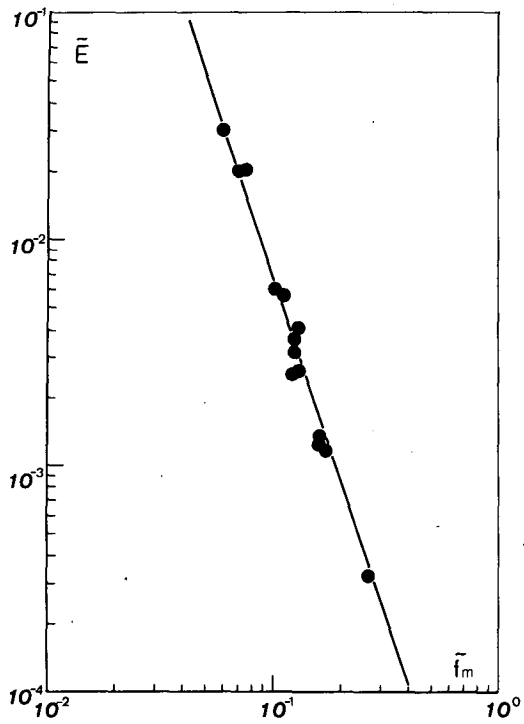

FIG. 4. Normalized wave energy $\tilde{E}$ ($\equiv g^2E/U^4$) versus the normalized spectral peak frequency $\tilde{f}_m$ ($\equiv Uf_m/g$). Solid line based on Eq. (11).

by Hasselmann *et al.* (1973). Recently, Pierson (1977) determined the fetch dependence of γ from a simple analysis of the spectral form of partially developed wind waves, though his result was not compared with measurements.

One of the main purposes of the present study is to determine the relation between γ and $\tilde{f}_m$ or γ and $\tilde{F}$. Before analyzing the spectral data, some preliminary considerations of the JONSWAP spectrum will be given below.

The total energy E of the JONSWAP spectrum is obtained from (3) as

$$E = \int_0^\infty \phi(f)df = \alpha g^2(2\pi)^{-4} \int_0^\infty f^{-5} \times \exp[-\tfrac{5}{4}\hat{f}^{-4}]\gamma^{\exp[-(f/f_m-1)^2/2\sigma^2]}\, df = \alpha g^2(2\pi)^{-4} f_m^{-4} \int_0^\infty \psi(\hat{f},\gamma,\sigma)d\hat{f}, \quad (16)$$

where

$$\hat{f} = f/f_m, \quad (17)$$

$$\psi(\hat{f},\gamma,\sigma) = \hat{f}^{-5} \exp[-\tfrac{5}{4}\hat{f}^{-4}]\gamma^{\exp[-(f/f_m-1)^2/2\sigma^2]}. \quad (18)$$

If we put

$$\int_0^\infty \psi(\hat{f},\gamma,\sigma)d\hat{f} = I(\gamma,\sigma) = 1/A(\gamma,\sigma), \quad (19)$$

Eq. (16) can be written as

$$E = \alpha g^2(2\pi)^{-4} f_m^{-4}/A(\gamma,\sigma), \quad (20)$$

or α is given by

$$\alpha = (2\pi)^4 E f_m^4 g^{-2} A(\gamma,\sigma). \quad (21)$$

By using the dimensionless variables in (10), the relation (21) can be rewritten as

$$\alpha = (2\pi)^4 \tilde{E} \tilde{f}_m^4 A(\gamma,\sigma). \quad (22)$$

The integration of (19) for $\gamma = 1$ gives $A(\gamma,\sigma) = 5$ irrespective of σ. Although the analytical integration of (19) for $\gamma > 1$ is difficult, numerical integration of (19) for various γ with fixed σ by relation (4) gives the approximate relation

$$A(\gamma,\sigma) = 5\gamma^{-1/3}, \quad 1 \leq \gamma < 4. \quad (23)$$

On substituting (11) and (23) into (22), the latter becomes

$$\alpha = 5.35 \times 10^{-2} \tilde{f}_m \gamma^{-1/3} \quad (24)$$

or

$$\gamma = 1.53 \times 10^{-4} \tilde{f}_m^3 \alpha^{-3}. \quad (25)$$

The similarity relation (25) will be used later to determine the dependence of the shape parameter γ on $\tilde{f}_m$.

Another shape parameter λ defined by Hasselmann *et al.* (1973) as $Ef_m^4/\alpha g^2$ can be expressed from (21) and (23) as

$$\lambda = (2\pi)^{-4}\gamma^{1/3}/5. \quad (26)$$

Hasselmann *et al.* (1976) assumed $\lambda = 1.6 \times 10^{-4}$ as a mean JONSWAP value. According to (26) this value corresponds approximately to λ for $\gamma = 2$.

c. *Determination of α and γ from the spectral data*

The values of α and γ are determined from the measured wave spectra in the same way as in Hasselmann *et al.* (1976). First, α is computed by

$$\alpha = (0.65 f_m)^{-1} \int_{1.35 f_m}^{2 f_m} (2\pi)^4 f^5 g^{-2} \times \exp\left[\frac{5}{4}\left(\frac{f}{f_m}\right)^{-4}\right]\phi(f)df, \quad (27)$$

and γ by

$$\gamma = \phi(f_m)(2\pi)^4 f_m^5 \exp(5/4)(\alpha g^2)^{-1}, \quad (28)$$

where the value of α determined from (27) is used for the computation of γ. The values of σ are not tested in our present study, and we use the mean JONSWAP value $\sigma = 0.07$ for $f \leq f_m$ and $\sigma = 0.09$ for $f > f_m$. Finally, the spectrum of the JONSWAP type (3) is compared to the measured spectra using the values of α and γ determined by (27) and (28), respectively.

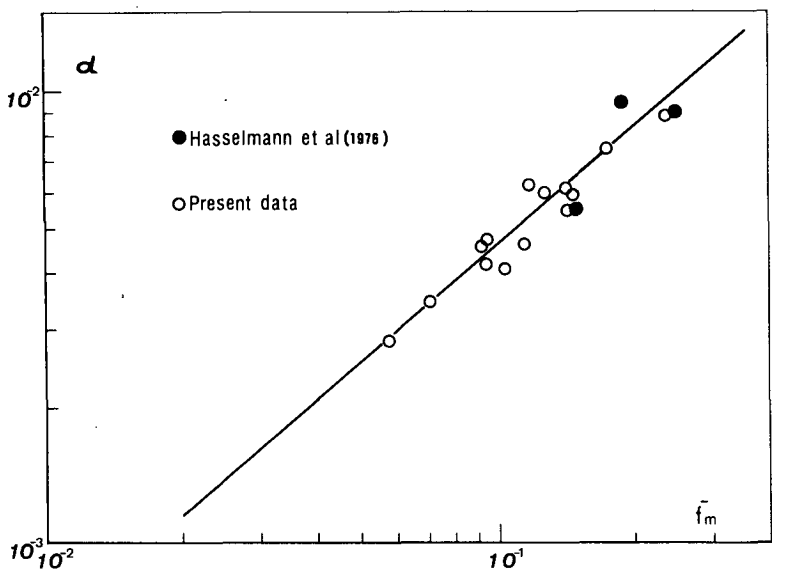

FIG. 5. The scale parameter α versus the normalized spectral peak frequency $\tilde{f}_m$.

4. Results and discussion

a. Similarity form of the wave spectra

Figs. 2 and 3 show typical examples of the measured wave spectra compared with the spectral form of the JONSWAP type, where the parameters α and γ are determined by (27) and (28), respectively, and mean JONSWAP values of σ are used. In these figures the power spectrum $\phi(f)$ is shown in the upper left, its dimensionless form $\phi f^5/g^2 = \tilde{\phi}(f/f_m)$ in the lower left, and another dimensionless form $\phi f_m/E = \hat{\phi}(f/f_m)$ in the upper right (in linear scale) and in the lower right (in log-linear scale). As can be seen from these figures, our measured spectra can be described quite well by the spectral form of the JONSWAP type.

b. Relation between $\tilde{E}$ and $\tilde{f}_m$ and effective wind speed U_e

Fig. 4 shows the relation between $\tilde{E}$ ($\equiv g^2E/U^4$) and $\tilde{f}_m$ ($\equiv Uf_m/g$) of our measured data, where a straight line is the empirical relation (11). As shown in the figure the present data agree very well with the empirical relation (11). The good agreement assures us of meaningful estimates of the effective wind speed U_e in the generation area by using (12) and the observed E and f_m. The effective wind speeds U_e thus obtained are shown in Table 1. Agreements between U and U_e are fairly good, though some differences of the order ±30% are found. Such differences can be attributed to various sources. Wave data of different series were obtained on different cruises using different observation ships. Anemometer heights of these ships are roughly 10 m but differ slightly from one to another. This may introduce some systematic deviations of the wind speed. On the other hand, the wind speed measured on a ship at a particular observation site is not necessarily representative of the effective wind speed in the entire generation area. In consideration of these situations, the estimated wind speed U_e (dropping the suffix e) will be used in the following analysis of the spectral data. It has been confirmed that the general trend of the results remains unaltered if the measured wind speed U is used instead of U_e, though the former introduces more scatter of the data than the latter.

c. Relations of α and γ to $\tilde{f}_m$

Fig. 5 shows the relation between the scale parameter α and the dimensionless frequency $\tilde{f}_m$ of the spectral peak. The straight line in the figure,

$$\alpha = 3.26 \times 10^{-2}\tilde{f}_m^{6/7}, \tag{29}$$

is the best fit to the data.

On substituting (29) into (25) we obtain the shape parameter γ as

$$\gamma = 4.42\tilde{f}_m^{3/7}. \tag{30}$$

This relation (30) is compared in Fig. 6 with the measured data. Agreements between (30) and the data are satisfactory. It is also interesting that, from (29) and (30), the relation between α and γ is given by

$$\alpha = 1.67 \times 10^{-3}\gamma^2. \tag{31}$$

The relation (29) is slightly different from that obtained by Hasselmann *et al.* (1976), i.e.,

$$\alpha = 3.3 \times 10^{-2}\tilde{f}_m^{2/3}. \tag{32}$$

However, the relation (29) obtained here fits fairly

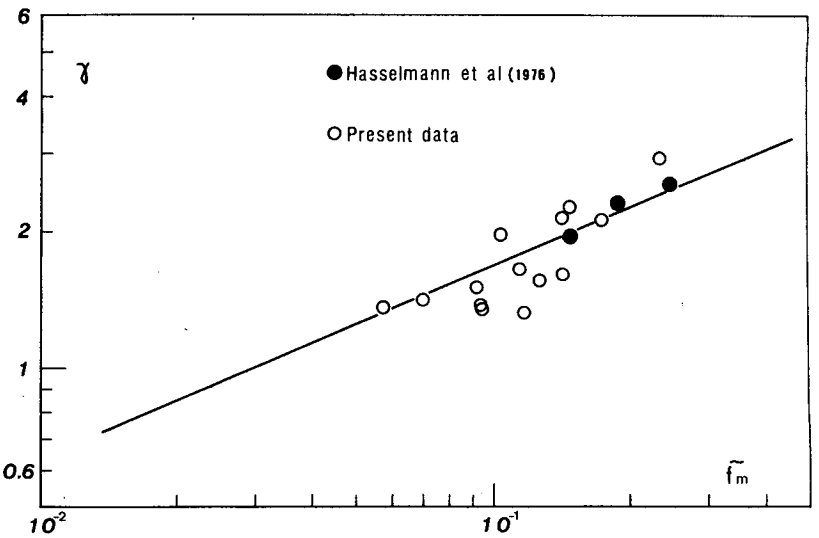

FIG. 6. The shape parameter γ versus the normalized spectral peak frequency $\tilde{f}_m$.

well to their original data shown in Fig. 9 of Hasselmann *et al.* (1976). The same can be said on the relation (30) for γ; their data for γ, shown in Fig. 2 of Hasselmann *et al.* (1976), scatter approximately around (30).

d. Fetch relations for α and γ

It is very difficult to determine the dimensionless fetch $\tilde{F}$ in the open ocean, because the boundary of a generation area of the wind waves is not always clear and the wind speed and direction are not uniform in a generation area. In order to determine the dimensionless fetch $\tilde{F}$ under such conditions, we introduce an effective dimensionless fetch $\tilde{F}_e$ (hereafter the suffix e will be dropped) in the following way. For wind waves at clearly defined finite fetch, e.g., wind waves in a bay or in a lake, many observations support the fetch relation of the form (6) or (9) for f_m very well (Mitsuyasu, 1968; Liu, 1971; Hasselmann *et al.*, 1973). On the basis of this fact, we determine the effective dimensionless fetch $\tilde{F}$ from the measured data of $\tilde{f}_m$ by assuming the relation (9) to be a universal relation. Although we can also utilize the fetch relation (8) for $\tilde{E}$ to estimate $\tilde{F}$, Eq. (9) is considered to be the more reliable.

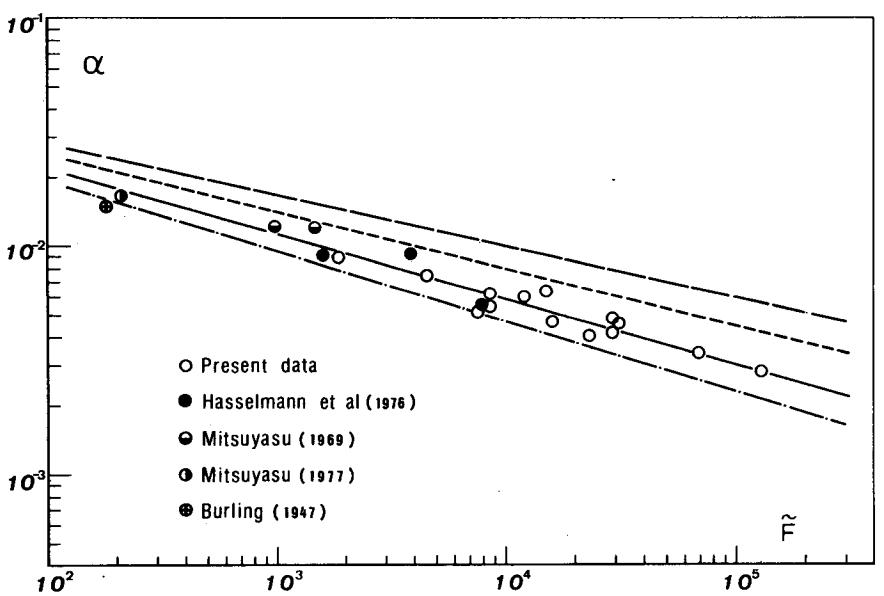

FIG. 7. The scale parameter α versus the dimensionless fetch $\tilde{F}$ ($\equiv gF/U^2$). Solid line based on Eq. (33); long dashed line Hasselmann *et al.* (1973); short dashed line Liu (1971); dot-dashed line Mitsuyasu (1973).

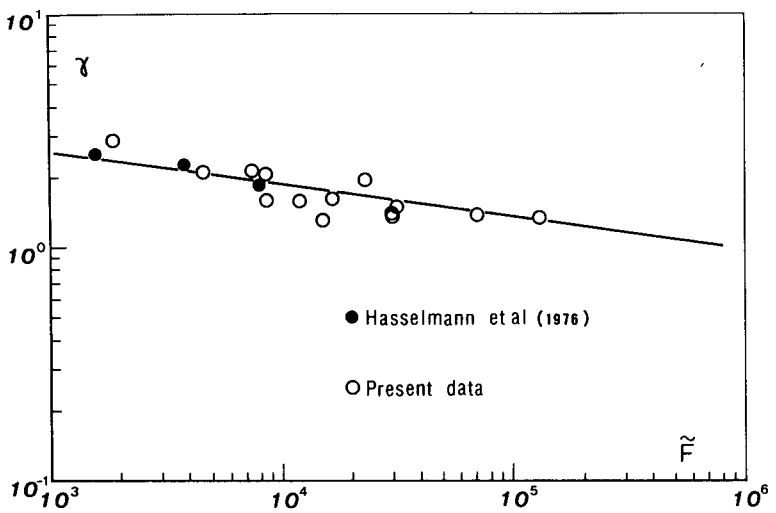

FIG. 8. The shape parameter γ versus the dimensionless fetch $\tilde{F}$.

It should be mentioned, however, that wind waves will gradually approach a saturated state for very long fetch, and that fetch relations (8) and (9) must be modified for such long fetch. In fact, such properties of wind waves at extremely long fetch were taken into account in the empirical formula IV derived by Wilson (1965). However, as can be seen from the original data shown in Fig. 16 of Wilson (1965), the approximate forms (8) and (9) for the fetch relations are well satisfied even for large fetch ($\tilde{F} \leqslant 10^5$). The present values of the dimensionless fetch $\tilde{F}$ determined from (9) by the data of $\tilde{f}_m$ are listed in Table 1, which shows that the estimated values of $\tilde{F}$ are smaller than 10^5 for many cases. Although we have tested for Wilson's formula IV to estimate $\tilde{F}$ from $\tilde{f}_m$, the estimated values show considerable scatter and consistent results have not been obtained. Therefore, the dimensionless fetch $\tilde{F}$ estimated from (9) will be used in the following analysis of the data.

Now from Eqs. (29) and (30), using the fetch relation (9), we obtain

$$\alpha = 8.17 \times 10^{-2} \tilde{F}^{-2/7}, \tag{33}$$

$$\gamma = 7.0 \tilde{F}^{-1/7}. \tag{34}$$

Relation (33) is compared in Fig. 7 with the measured data. Fig. 7 also shows various empirical formulas previously reported:

$$\alpha = 8.1 \times 10^{-2} \tilde{F}^{-0.308} \quad \text{(Mitsuyasu, 1973)} \tag{35}$$

$$\alpha = 8 \times 10^{-2} \tilde{F}^{-0.25} \quad \text{(Liu, 1971)} \tag{36}$$

$$\alpha = 7.6 \times 10^{-2} \tilde{F}^{-0.22} \quad \text{(Hasselmann } et\ al.\text{, 1973).} \tag{37}$$

In order to confirm the present formula we have also shown in Fig. 7, the previous data of α reported by various authors (Burling, 1959; Mitsuyasu, 1969, 1977; Hasselmann *et al.*, 1976). It can be seen from Fig. 7 that the formula (33) shows the best overall fit to the data, although the various relations (35), (36) and (37) are similar to one another.

The fetch relation (34) for γ is compared in Fig. 8 with the measured data. In Fig. 8 the data obtained by Hasselmann *et al.* (1976) are also included. Agreement between (34) and various data is satisfactory, and γ approaches ~ 1 near $\tilde{F} = 10^6$, though the relation (9) may not be reliable in this extrapolated range.

5. Further discussion

a. Other spectral forms of ocean waves

In the present study, the spectral form of JONSWAP type has been *a priori* used in the

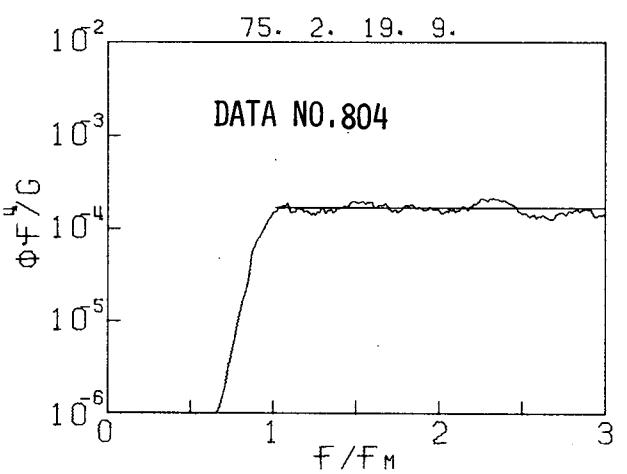

FIG. 9. The normalized form of power spectrum for ocean wave data set No. 804. The straight line is based on Eq. (38) with the best fit value of α'.

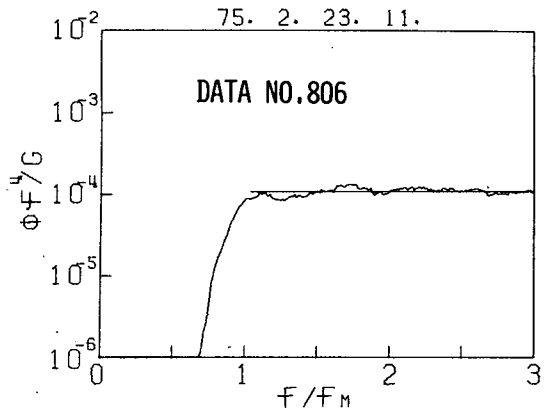

FIG. 10. As in Fig. 9 except for ocean wave data set No. 806.

analysis of observed wave spectra. Consistent results have been obtained as discussed in the preceeding section. However, several other spectral forms have been presented as similarity forms of ocean wave spectra. Among others, Toba (1973, 1978) recently proposed the following form for the high-frequency range of the wave spectrum:

$$\phi(f) = \alpha'(2\pi)^{-3} g u_* f^{-4}, \quad f > f_m, \tag{38}$$

where α' is a dimensionless constant. This form is compared with our present data, and typical examples are shown in Figs. 9 and 10. In spite of the apparent difference between the spectral forms (3) and (38), the form (38) also fits quite well to the observed spectra at the high-frequency side of the spectrum ($f_m \leqslant f \leqslant 2f_m$). The dimensionless constant α' shows a fairly constant value for all data analysed; its mean value is $\alpha' = 8.7 \times 10^{-2}$. However, closer examination of the data shows a trend of fetch dependence of α', which will be discussed later.

The spectral data compared in Figs. 9 and 10 with the spectral form (38) are the same in Figs. 2 and 3. Therefore, the present results show that typical spectra of ocean waves can be expressed by two quite different spectral forms [(3) and (38)] as far as the spectral form at high-frequency side ($f_m \leqslant f \leqslant 2f_m$) is concerned. This problem will be discussed below.

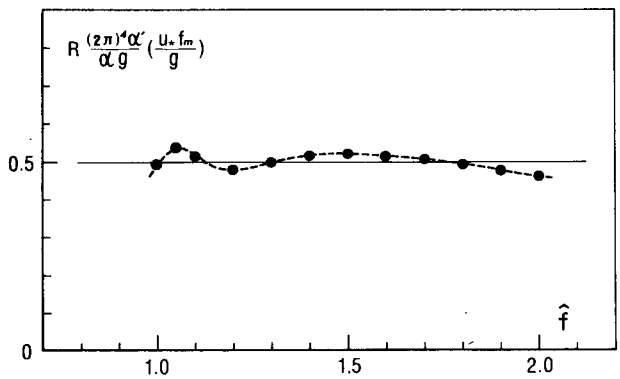

FIG. 11. The function in braces of Eq. (39) for $1 \leqslant \hat{f}\ (= f/f_m) \leqslant 2$.

b. The relation between the JONSWAP spectrum and the spectral form (38)

At high frequencies ($f > f_m$), the ratio R of the JONSWAP spectrum (3) to the spectral form (38) is given by

$$R = \frac{\alpha}{\alpha'} g(2\pi)^{-1} u_*^{-1} f^{-1} \exp[-\tfrac{5}{4} f^{-4}] \gamma^{\exp[-(f/f_m-1)^2/2\sigma^2]}$$

$$= \frac{\alpha g}{2(\pi)\alpha'} \left(\frac{u_* f_m}{g}\right)^{-1} \times \{\hat{f}^{-1} \exp[-\tfrac{5}{4}\hat{f}^{-1}] \gamma^{\exp[-(f/f_m-1)^2/2\sigma^2]}. \tag{39}$$

The functional form in the right-hand braces is shown in Fig. 11 for the case $\sigma = 0.09$ and $\gamma = 1.7$. As can be seen from the figure, the function in the braces takes a nearly constant value, 0.5, in a frequency range $1 \leqslant \hat{f} \leqslant 2$.[2] This is consistent with fact that the apparently different spectral forms (3) and (38) fit the same spectral data if the dimensionless constants α and α' are appropriately determined. The meaning of this result is as follows; at high frequencies $f > 2f_m$, the JONSWAP spectrum approaches to the equilibrium spectrum proportional to f^{-5} (Phillips, 1958) but at frequencies $f_m < f < 2f_m$, it is approximately proportional to f^{-4} due to the effects of terms $\exp[-1.25(f/f_m)^{-4}]$ and $\gamma^{\exp[-(f/f_m-1)^2/2\sigma^2]}$.

Now, rearranging (39) by taking $R = 1$ and using a value of 0.5 for the term in braces, yields

$$\alpha' = 0.5(2\pi)^{-1}\alpha\,(u_* f_m/g)^{-1}. \tag{40}$$

On substituting (29) and assuming $u_* = U/25$, Eq. (40) reduces to

$$\alpha' = 6.49 \times 10^{-2} \tilde{f}_m^{-1/7}. \tag{41}$$

With the further substitution of (9), Eq. (41) becomes

$$\alpha' = 5.57 \times 10^{-2} \tilde{F}^{1/21}. \tag{42}$$

Fig. 12 show formula (42) compared with the observed values of α', where the data obtained by Kawai *et al.* (1977) are included as additional data for relatively short fetch.

As shown in Fig. 12, the empirical relation (42) for α' fits quite well to our observed data as well as to the previous data obtained by Kawai *et al.* (1977). From (42) and Fig. 12 we can conclude that constant α' in (38) depends on the dimensionless fetch $\tilde{F}$, though its dependence on $\tilde{F}$ is very weak and

[2] Since the effect of γ on the spectral form is negligible for a frequency region $\hat{f} \geqslant 1.2$, the conclusion holds for a region $1.2 \leqslant \hat{f} \leqslant 2.0$ irrespective of the values of γ or σ.

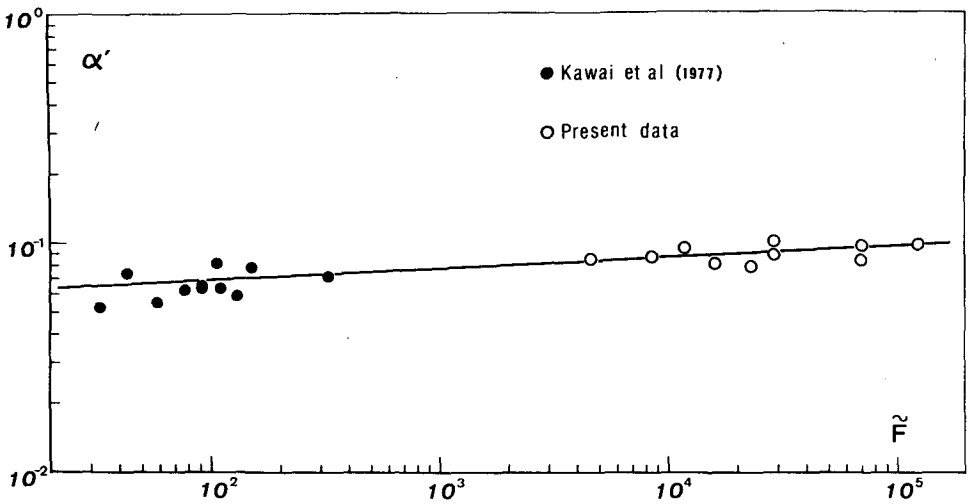

FIG. 12. The scale parameter α' versus dimensionless fetch $\tilde{F}$.

α' can be approximated as constant for some limited range of $\tilde{F}$.

c. High-frequency wave spectrum

According to recent studies (Pierson and Stacy, 1973; Mitsuyasu and Honda, 1974; Mitsuyasu, 1977), there exists a high-frequency region of the wave spectrum in the gravity-capillary range where the frequency spectrum is given by the same form as (38), where g is replaced by $g_* (= g + \sigma_s k^2/\rho$, where σ_s is surface tension and ρ the density of water) to include the effect of surface tension (Toba, 1973). However, the dimensionless constant α' is smaller in the gravity-capillary range than that in the gravity range analyzed in the present study, and these two ranges of the wave spectrum need to be discussed separately. Further studies are required to clarify the transition range of the wave spectrum from the gravity range to the gravity-capillary range.

d. Swells and their coexistence with wind waves

In the present study only single-peaked spectra are selected for the analysis. However, there are many spectral data which show multiple-peaked form (Fig. 13). That is, wind waves coexist, in many cases, with the background swell, though their relative energy levels vary depending on the conditions. Conversely, it is difficult to pick up from the present data the spectral data of pure swell, because local wind waves have been superimposed on the swell in many cases, although their relative energy levels also vary. Therefore, we have been unable to determine the spectral form of the swell in this study.

The use of data where wind waves coexist with swell introduces considerable scatter of the parameters of the spectral forms (3). Therefore, wave data

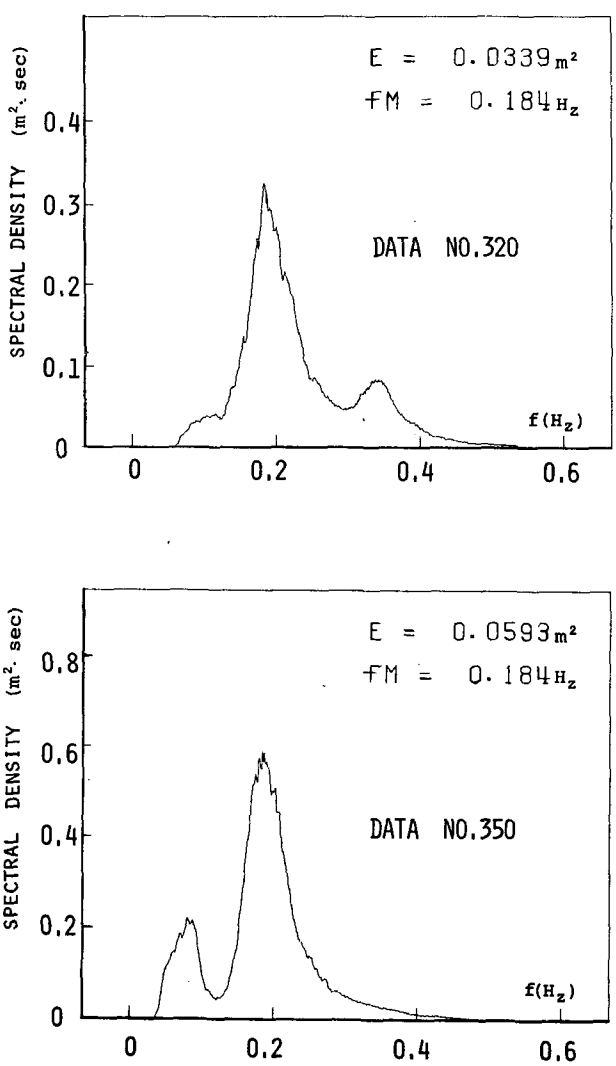

FIG. 13. Examples of multiple-peaked spectra of ocean waves.

contaminated by swell have been carefully eliminated from our present analysis because the purpose of the present study is to clarify the fundamental properties of the ocean wave spectra generated under simple conditions.

e. Some limitations of the present study

We wish to emphasize here two limitations of the present study:

1) The functional form (23) for $A(\gamma)$ is an approximate relation which is satisfied only in a range $1 \leqslant \gamma < 4$. Therefore, some modification should be necessary if we apply the present results to the spectral data of such a sharp spectral form as $\gamma > 4$, although most of the present data are in a range $\gamma < 4$.

2) In the derivation of the fetch relations for α and γ, we have used the fetch relation of $\tilde{f}_m$ for wind waves at relatively short fetches (9). Therefore, some modification will also be needed when the present results are applied to wave data at extremely large fetches, although the relations of α and γ to $\tilde{f}_m$ [(29) and (30)] are universal.

6. Conclusions

The following conclusions can be drawn from the present study:

1) A universal relation between the wave energy E and the spectral peak frequency f_m is confirmed to be valid for wind waves in the open ocean.

2) Spectral forms of ocean waves in generation area can be well represented by the spectral form of the JONSWAP type.

3) The shape parameter γ is clearly fetch dependent and the relation between γ and the dimensionless fetch $\tilde{F}$ ($\equiv gF/U^2$) is approximated by (34). The scale parameter α is also fetch dependent as reported previously, and the revised fetch relation for α is given by (33).

4) Observed wave spectra represented by the spectrum of the JONSWAP type also can be approximated by the different spectral form (38) proposed by Toba (1978) as far as the high-frequency side of the spectrum ($f \geqslant f_m$) is concerned. The reason for this is found to be in the similarity of both spectra as discussed in Section 5.

5) The dimensionless constant α' in the spectral form (38) is also fetch dependent, although its dependence on the dimensionless fetch $\tilde{F}$ is very weak as shown in (42).

Acknowledgments. We are grateful to Prof. Y. Toba, Prof. R. O. Reid and Dr. A. Masuda for their helpful comments on a first draft of this paper. We are also indebted to Mr. M. Tanaka and Mr. T. Morita for their assistance in computer analysis of the wave data and to Mr. K. Eto and Ms. M. Hojo for their assistance in preparing the manuscript. The work described in this paper is part of a special project supported by the Ministry of Education, Japan. Some additional wave data were obtained on a cruise for AMTEX which is a subproject of GARP.

REFERENCES

Burling, R. W., 1959: The spectrum of waves at short fetches. *Dtsch. Hydrogr. Z.*, **12,** 45–64, 96–117.

Hasselmann, K. *et al.*, 1973: Measurements of wind wave growth and swell decay during the Joint North Sea Wave Project (JONSWAP). *Dtsch. Hydrogr. Z.*, **A(8)** (Suppl), 95 pp.

Hasselmann, K., D. B. Ross, P. Muller and W. Sell, 1976: A parametric wave prediction model. *J. Phys. Oceanogr.*, **6,** 200–228.

Kawai, S., K. Okuda and Y. Toba, 1977: Field data support of three-seconds power law and $gu_*\sigma^4$-spectral form for growing wind waves. *J. Oceanogr. Soc. Japan*, **33,** 137–150.

Liu, P. C., 1971: Normalized and equilibrium spectra of wind waves on Lake Michigan. *J. Phys. Oceanogr.*, **1,** 249–257.

Mitsuyasu, H., 1968: On the growth of the spectrum of wind-generated waves (I). *Rep. Res. Inst. Appl. Mech., Kyushu Univ.*, **16,** 459–482.

——, 1969: On the growth of the spectrum of wind-generated waves (II). *Rep. Res. Inst. Appl. Mech., Kyushu Univ.*, **17,** 235–248.

——, 1973: One dimensional wave spectra at limited fetch. *Rep. Res. Inst. Appl. Mech., Kyushu Univ.*, **20,** 37–53.

——, 1977: Measurement of the high-frequency spectrum of ocean surface waves. *J. Phys. Oceanogr.*, **7,** 882–891.

——, and T. Honda, 1974: The high-frequency spectrum of wind-generated waves. *J. Oceanogr. Soc., Japan*, **30,** 185–198.

——, F. Tasai, T. Suhara, S. Mizuno, M. Ohkusu, T. Honda and K. Rikiishi, 1975: Observation of the directional spectrum of ocean waves using a cloverleaf buoy. *J. Phys. Oceanogr.*, **5,** 750–760.

Phillips, O. M., 1958: The equilibrium range in the spectrum of wind-generated waves. *J. Fluid Mech.*, **4,** 426–434.

Pierson, W. J., 1977: Comments on "A parametric wave prediction model." *J. Phys. Oceanogr.*, **7,** 127–134.

——, and L. Moskowitz, 1964: A proposed spectral form for fully developed wind seas based on the similarity theory of S. A. Kitaigorodskii. *J. Geophys. Res.*, **69,** 5181–5190.

——, and R. A. Stacy, 1973: The elevation, slope and curvature spectra of a wind roughened sea surface. NASA Contractor Rep. CR2247, Langley Research Center, 128 pp.

Toba, Y., 1972: Local balance in the air-sea boundary process I. *J. Oceanogr. Soc. Japan*, **28,** 109–120.

——, 1973: Local balance in the air-sea boundary process III. *J. Oceanogr. Soc. Japan*, **29,** 209–220.

——, 1978: Stochastic form of the growth of wind waves in a single-parameter representation with physical implications. *J. Phys. Oceanogr.*, **8,** 494–507.

Wilson, B. W., 1965: Numerical prediction of ocean waves in the North Atlantic for December, 1959. *Dtsch. Hydrogr. Z.*, **18,** 114–130.